Proc. Nat. Acad. Sci. USA
Vol. 72, No. 2, pp. 531–534, February 1975

X-Ray Diffraction Studies of Human Erythrocyte Membrane Structure

(small angle x-ray diffraction/red blood cell/hemoglobin)

JAMES B. STAMATOFF, SAMUEL KRIMM, AND NANCY REID HARVIE

Biophysics Research Division, Department of Physics, and Macromolecular Research Center, University of Michigan, Ann Arbor, Mich. 48105

Communicated by J. Lawrence Oncley, November 21, 1974

ABSTRACT **Small angle x-ray diffraction patterns have been obtained from ordered arrays of hemoglobin-free human erythrocyte membranes by use of improved techniques. Diffraction data have been recorded to 9 Å resolution on samples whose lattice periodicity was varied (by changing humidity) from 55.5 Å to 69.6 Å. The observed reflections permitted tracing the intensity transform of the membranes. Phases for the reflections were assigned by the minimum wavelength principle. An electron density profile was then obtained by Fourier inversion, and yielded a symmetric membrane about 55 Å in width. This structure can account for the previously reported diffuse scattering observed in other preparations (thus rendering unnecessary the proposed assignment of this scattering to a separated lipoprotein phase) and for the continuous scattering that we have recorded from isolated membranes in buffer. Lower resolution data that we have obtained from ultracentrifugally prepared lattices in buffer (and therefore without dehydration) are consistent with the above results, and support our view that we are observing diffraction from intact membranes.**

Small angle x-ray diffraction techniques have been used to investigate the erythrocyte membrane (1–7). The diffraction data that have been reported consist of three or four orders of ~110-Å periodicity for erythrocyte membranes that contain large amounts of hemoglobin and two orders of ~70-Å periodicity for hemoglobin-free erythrocyte membranes. These data are insufficient to determine phase angles of the reflections by swelling techniques (8), and thus do not permit computation of projected electron density distributions by Fourier inversion. We now report higher resolution x-ray diffraction data from hemoglobin-free human erythrocyte membranes and the computation of projected electron density distributions based upon an assignment of phase angles.

MATERIALS AND METHODS

Whole human blood, type O, Rh positive, was drawn into Fenwal JH-IN heparinized blood packs. Hemoglobin-free membranes were prepared by the procedure of Dodge *et al.* (9). Membranes were hemolyzed and washed with pH 7.4, 15 imOsm sodium phosphate buffer. The membranes were finally suspended in pH 6.3, 15 imOsm phosphate buffer and preserved by the addition of 0.5 mM NaN_3. The suspension was examined optically with a Leitz phase contrast microscope and showed a homogeneous preparation of membrane vesicles approximately 6 μm in diameter.

The amount of membrane material in the samples was determined using a modification of the dry weight method described by Hunter (10). A semi-microbalance, Mettler type H16, was used. Membrane samples were measured with class A volumetric pipettes followed by a rinse of the pipette with glass-distilled water into the weighing bottle. The temperature of the vacuum oven was 70° for the second 24-hr period. Dry weights, done in triplicate, were calculated on a weight per volume basis.

Total protein was measured by the method of Lowry *et al.* (11), with bovine serum albumin as a standard. Hemoglobin was determined by a pyridine hemochromagen method (12), with human hemoglobin (Sigma Chemical Co.) as a standard. *N*-Acetylneuraminic acid (NeuNAc) was measured by the method of Warren (13), with purified NeuNAc (Sigma Chemical Co.) as a standard.

Membrane samples were prepared for x-ray diffraction by centrifugation at $10^5 \times g$ for 24 hr in a Spinco model L ultracentrifuge using a SW 39 rotor at 4°. The pellets were equilibrated in a nitrogen atmosphere at 37° and 93–98% relative humidity. The pellets were cut into strips, mounted in the x-ray diffraction chamber, and equilibrated in a water vapor atmosphere at 4° and 75–100% relative humidity before exposure.

Diffraction patterns were recorded with a Rigaku Denki RU-3H rotating anode generator, a mirror-monochromator point focusing arrangement, and an evacuated curved Guinier camera. The incident beam measured 2 mm × 0.5 mm at the specimen and 0.1 mm × 0.3 mm at the film. The sample-to-film distance was 126.8 mm. Patterns were recorded on Ilford Industrial-G x-ray film with approximately a 48-hr exposure and usually within 1 week after the blood was drawn. Intensities and spacings were measured from densitometer traces recorded on a Joyce-Loebl MK IIIC microdensitometer.

In certain experiments, erythrocyte membranes were incubated with neuraminidase (Worthington Biochemical Corp.) and bound with hemoglobin contained in the erythrocyte hemolysate or with poly(L-lysine) (Sigma Chemical Co.). The membranes were incubated with the enzyme at a concentration of 20 μg/mg of membrane protein at 37° for 1 hr in pH 6.3, 15 imOsm sodium phosphate buffer. The samples were then cooled to 4° with ice water and washed twice with pH 6.3, 15 imOsm sodium phosphate buffer using a 1:11 washing ratio. Release of NeuNAc was verified by assay of the supernatants and acid hydrolysates of the washed membranes.

The neuraminidase-treated membranes were bound with hemoglobin or poly(L-lysine) as follows: The first hemolysate in the preparation of the stroma was dialyzed at pH 6.3, 15

Abbreviation: NeuNAc, *N*-acetylneuraminic acid.

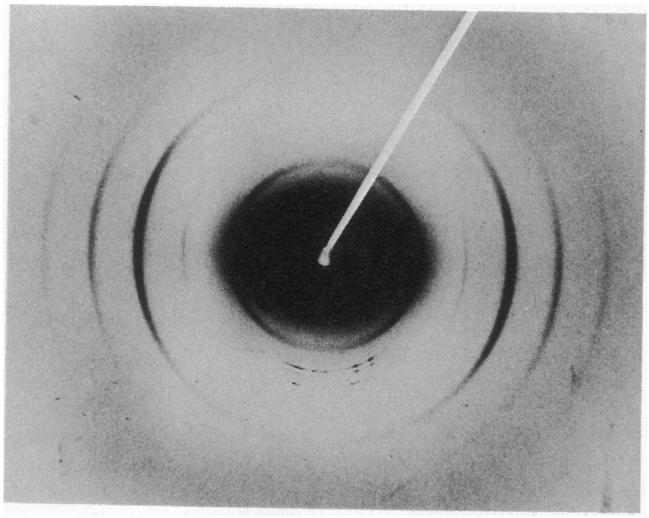

FIG. 1. An example of an x-ray diffraction pattern recorded from hemoglobin-free human erythrocyte membranes. The periodicity is 59.0 Å and the sample was in equilibrium with 98% relative humidity at 4°. The reflections are oriented along an axis parallel to the ultracentrifugation axis and perpendicular to the plane of the membrane. The first two orders are overexposed in order to display higher orders of diffraction.

imOsm sodium phosphate buffer. Equal volumes of the dialyzed hemolysate (about 7 mg of hemoglobin per ml) and neuraminidase-treated stroma (about 5 mg/ml) were combined and incubated at 4° for 1 hr. The membranes were then washed three times with 210 ml of pH 6.3, 15 imOsm sodium phosphate buffer. The resulting stroma were red and visibly aggregated.

Poly(L-lysine), molecular weight about 4×10^5, was dissolved in glass-distilled water at a concentration of 20 mM (monomer weight). The solution was dialyzed exhaustively against glass-distilled water after which 0.45 ml was added to 4 ml of a neuraminidase-treated membrane suspension (about 2.5 mg/ml). The membranes were visibly aggregated after the addition of the polymer.

The neuraminidase-treated membranes, bound to hemoglobin or poly(L-lysine), were centrifuged at $10^5 \times g$ for 24 hr into a 1-mm thick Lucite chamber fitted with two 0.076-mm

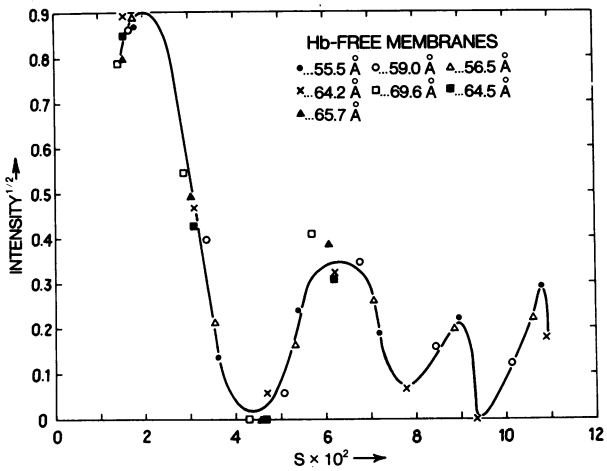

FIG. 2. The square root of the intensities for hemoglobin-free erythrocyte membranes plotted against the reciprocal space variable S(Å^{-1}).

TABLE 1. *Protein, hemoglobin, and N-acetylneuraminic acid of hemoglobin-free erythrocyte membrane preparations*

% Non-Hb* protein	% Hb†	mol of NeuNAc / mg of Hb corrected dry weight	Hb/non-Hb protein
41.9	2.6	55.5	0.06
43.9	1.4	—	0.03
37.4	2.0	—	0.05
43.3‡	1.5‡	9.6‡	0.04‡

* % = (total protein − hemoglobin)/(dry weight − hemoglobin) × 100.
† % = hemoglobin/(dry weight − hemoglobin) × 100.
‡ Neuraminidase-treated membranes.

thick cellulose acetate x-ray windows. The diffraction experiment was conducted at room temperature with an exposure of 24 hr. A layer of buffer was maintained on top of the condensed membrane pellet during the exposure.

RESULTS

The results of the biochemical analysis of the membrane samples are given in Table 1. The percent non-hemoglobin protein and percent hemoglobin were based upon the hemoglobin corrected dry weight of the total membrane material.

An example of the diffraction patterns that were recorded is shown in Fig. 1. Seven sets of data were recorded for seven different periodicities from 55.5 Å to 69.6 Å. The spacing was altered by varying the water content of the specimen. Four to seven orders of diffraction were recorded for each set of data. The minimum Bragg spacing was 9 Å. Diffuse scattering about the beam stop was negligible when compared to the intensity of the first order.

Integrated intensities were approximated by evaluating the product of the maximum and half-width of each reflection. The intensities were corrected for arcing by multiplying each value by $h \cdot \sin 4\theta$, where h is the order of the reflection and 2θ is the scattering angle. This correction, applicable for the curved Guinier camera, is essentially identical with the h^2 factor of Wilkins *et al.* (14) in the small-angle region. One set of data was scaled with respect to another using the relation (15),

$$\frac{1}{d_1}\sum_{h=1}^{N} I(h/d_1) = \frac{1}{d_2}\sum_{h=1}^{N} I(h/d_2)$$

where d_1 and d_2 are the respective Bragg spacings and N is the number of orders of diffraction. The square root of the intensities could then be plotted as a function of the reciprocal space variable, $S = (2 \sin \theta)/\lambda$, as shown in Fig. 2. The smooth curve that results from this plot indicates that the reciprocal lattice is sampling one continuous function which is the Fourier transform of the unit cell contents.

The vesicles were prepared by methods reported not to fragment the membranes (9). Assuming that the electron density of the double membrane pair projected on an axis perpendicular to the membrane surface is symmetric, the resulting Fourier transform must be real. Therefore, the phase angles that are required for the reconstruction of the projected electron density distribution are 0 or π. Based upon the general periodicity of the curve shown in Fig. 2 and the minimum wavelength principle of Bragg and Perutz (16), it appears

very probable that all of the maxima are of the same sign except the third. If we assign a positive value to the third maximum and negative values to all of the rest, projected electron density distributions may be obtained from the reflections, as shown in Fig. 3. The scale factors are slightly different from those used in Fig. 2. The change in scale factor is the result of applying a rigorous method of phase angle determination (17).

Examples of diffraction patterns recorded from neuraminidase-treated erythrocyte membranes are shown in Fig. 4. Fig. 4a shows a diffraction pattern from neuraminidase-treated, hemoglobin-rebound membranes in sodium phosphate buffer. The Bragg spacing of the first order is 113 Å. Fig. 4b shows a diffraction pattern from neuraminidase-treated, poly(L-lysine)-bound membranes in sodium phosphate buffer with a first-order Bragg spacing of 67 Å.

DISCUSSION

The minimum wavelength principle that was used to obtain phase angle information is not rigorous (18). However, the same phase angle assignments have been shown to be valid, based upon comparison of electron densities by a rigorous method (ref. 17; Stamatoff and Krimm, to be published) in which one electron density distribution generated from one set of reflections was plotted against another electron density distribution generated from another set of reflections for all possible combinations of phase angles. Therefore, we identify the projected electron density distributions with the unit cell contents.

The width of the structure is approximately 55 Å. The structure is symmetric and could represent either two asymmetric membranes that are each approximately 27.5 Å wide or one symmetric membrane that is 55 Å wide. In comparison with other membrane structures (19) or lipid bilayers (20), a width of 27.5 Å would be unreasonable. Therefore, it is concluded that the projected electron density distribution of the hemoglobin-free human erythrocyte membrane is symmetric at 9-Å resolution within our ability to record diffracted intensity. The symmetry that has been determined does not imply symmetry for the three-dimensional structure of the membrane, nor does it imply biochemical symmetry. Furthermore, if there is a small asymmetric component of the projected electron density distribution, it could be undetectable due to a combination of heterogeneity of the membrane population (e.g., variations due to the age of the erythrocyte) and small lattice disorders. Small asymmetries would produce weak odd-order reflections of a periodicity precisely double that which was observed.

The proposal that membrane components can separate due to dehydration (7) would imply that the above projected electron density distributions are not those of an intact membrane. The periodicity of the diffraction pattern recorded from poly(L-lysine)-bound, neuraminidase-treated erythrocyte membranes indicates, however, that the membrane is thinner than the suggested width of 112 Å (3). Assuming that membranes are separated by a monomolecular layer of poly(L-lysine) and using the 55-Å thickness of the structure determined for partially dehydrated membrane samples, this layer would be about 12 Å thick, a reasonable diameter of an α-helix [the conformation expected for poly(L-lysine) at the pH used]. This pattern was recorded in buffer, so that there is no possibility of separation of membrane components due to

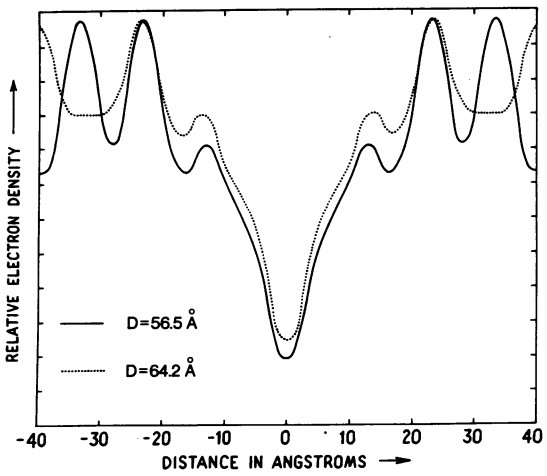

FIG. 3. Projected electron density distributions for hemoglobin-free human erythrocyte membranes obtained by Fourier inversion of two different sets of reflections. The signs of the reflections were (− − − − + − −) for orders h = 1–7 for the periodicity 64.2 Å and (− − − − + −) for orders h = 1–6 for the periodicity 56.5 Å. The scale factor of the reflections was slightly different from that used in Fig. 2 and was obtained by a rigorous method of phase determination (see ref. 17). The curves were plotted by a computer using a line printer. A smooth curve was drawn through these plots. The structure is approximately 55 Å wide; edges of neighboring unit cells are shown for each periodicity.

dehydration. In addition, the random orientation of this pattern indicates that the membrane lattice was formed by aggregation prior to ultracentrifugation. Thus, fusion of membranes due to ultracentrifugation is unlikely.

The previously proposed thickness of 112 Å for the membrane (3) was based upon the periodicity observed for partially dehydrated membrane samples that were bound with large quantities of hemoglobin. The periodicity of the diffraction pattern that we have recorded from hemoglobin-bound, neuraminidase-treated erythrocyte membranes is essentially the same as that reported previously (7). These and other similar experiments (17) indicate that the projected electron density distributions are those of an intact, hemoglobin-free erythrocyte membrane.

We have been able to show that the diffuse scattering previously observed and attributed to a residual lipoprotein phase (7) can be mathematically reproduced by considering the effects of lattice distortion and using the electron density

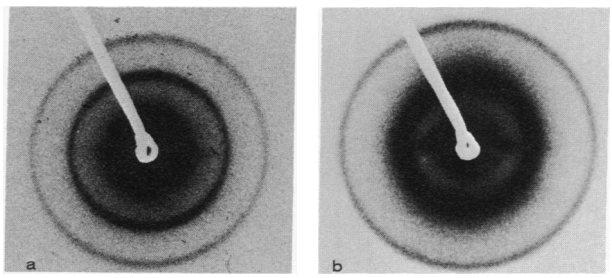

FIG. 4. X-ray diffraction patterns of neuraminidase-treated, hemoglobin-free human erythrocyte membranes in pH 6.3, 15 imOsm sodium phosphate buffer. (a) Bound with hemoglobin, periodicity = 113 Å. (b) Bound with poly(L-lysine), periodicity = 67 Å.

distribution shown in Fig. 3 (17). We have experimentally determined that the intensity of the diffuse scattering is dependent upon the rate of partial dehydration (17). We have also obtained a scattering curve essentially identical to that determined by Wilkins *et al.* (14) for dispersions of hemoglobin-free erythrocyte membranes. The continuous intensity curve computed from the projected electron density distribution shown in Fig. 3 is approximately the same as the experimentally recorded intensity curve (17), thus indicating that the membrane structures in the dispersion and in the oriented pellet are essentially the same.

The projected electron density distribution is consistent with the fluid mosaic model of membrane structure proposed by Singer and Nicolson (21). The width of the membrane compares favorably with that determined by Peters (22) using energy transfer methods. Models in which all of the protein is on either or both sides and is excluded from the interior of a lipid bilayer are inconsistent with the width of the membrane, the protein content, and shape of the electron density distribution. Although other models are possible, the shape of the electron density distribution is indicative of the presence of phospholipids in a bilayer arrangement.

J.B.S. was supported by a Macromolecular Research Center Fellowship. This work was supported in part by funds from the University of Michigan Cancer Research Committee, National Science Foundation Grant GB-15682 (S.K.), and by National Institutes of Health Grant HL-09739 (N.R.H.).

1. Finean, J. B., Coleman, R., Green, W. G. & Limbrick, A. R. (1966) *J. Cell Sci.* **1**, 287–296.
2. Finean, J. B., Coleman, R., Knutton, S., Limbrick, A. R. & Thompson, J. E. (1968) *J. Gen. Physiol.* **51**, 195–255.
3. Finean, J. B. (1969) *Quart. Rev. Biophys.* **2**, 1–23.
4. Finean, J. B. (1972) *Chem. Phys. Lipids* **8**, 279–284.
5. Finean, J. B. (1973) *Bicchem. Soc. Trans.* **1**, 327–329.
6. Coleman, R., Finean, J. B., Knutton, S. & Limbrick, A. R. (1970) *Biochim. Biophys. Acta* **219**, 81–92.
7. Knutton, S., Finean, J. B., Coleman, R. & Limbrick, A. R. (1970) *J. Cell Sci.* **7**, 357–371.
8. Worthington, C. R., King, G. I. & McIntosh, T. J. (1973) *Biophys. J.* **13**, 480–494.
9. Dodge, J. J., Mitchell, C. & Hanahan, D. J. (1963) *Arch. Biochem. Biophys.* **100**, 119–130.
10. Hunter, M. J. (1966) *J. Phys. Chem.* **70**, 3285–3292.
11. Lowry, O. H., Rosebrough, H. J., Farr, A. L. & Randall, R. J. (1951) *J. Biol. Chem.* **193**, 265–275.
12. Paul, K. G., Theorell, H. & Akeson, A. (1953) *Acta Chem. Scand.* **7**, 1284–1287.
13. Warren, L. (1959) *J. Biol. Chem.* **234**, 1971–1975.
14. Wilkins, M. H. F., Blaurock, A. E. & Engleman, D. M. (1971) *Nature New Biol.* **230**, 72–76.
15. Blaurock, A. E. (1967) Ph.D. Dissertation, University of Michigan.
16. Bragg, W. L. & Perutz, M. F. (1952) *Proc. Roy. Soc. Ser. A* **213**, 425–435.
17. Stamatoff, J. B. (1974) Ph.D. Dissertation, University of Michigan.
18. Perutz, M. F. (1954) *Proc. Roy. Soc. Ser. A* **225**, 264–286.
19. McIntosh, T. J. & Worthington, C. R. (1974) *Biophys. J.* **14**, 363–386.
20. Lesslauer, W., Cain, J. E. & Blasie, J. K. (1972) *Proc. Nat. Acad. Sci. USA* **69**, 1499–1503.
21. Singer, S. J. & Nicolson, G. L. (1972) *Science* **175**, 720–731.
22. Peters, R. (1973) *Biochim. Biophys. Acta* **330**, 53–60.